Journal of Molecular Graphics and Modelling 51 (2014) 1–6

Contents lists available at ScienceDirect

Journal of Molecular Graphics and Modelling

journal homepage: www.elsevier.com/locate/JMGM

Boosting sensitivity of boron nitride nanotube (BNNT) to nitrogen dioxide by Fe encapsulation

Yu-qing Zhang [c], Yue-Jie Liu [a], Yan-ling Liu [b,*], Jing-xiang Zhao [a,*]

[a] Key Laboratory for Photonic and Electronic Bandgap Materials, Ministry of Education, Harbin Normal University, Harbin 150025, China
[b] College of Chemistry and Chemical Engineering, Hainan Normal University, Haikou 571158, China
[c] College of Teacher Education, Harbin Normal University, Harbin 150025, China

ARTICLE INFO

Article history:
Accepted 5 April 2014
Available online 18 April 2014

Keywords:
NO_2 sensor
BNNT
Fe encapsulation
DFT

ABSTRACT

The pristine boron nitride nanotube (BNNT) exhibits a poor chemical reactivity to some adsorbates, thus greatly limiting its application for the gas sensor. In the present work, using density functional theory (DFT) methods, we put forward a novel strategy to enhance the sensitivity of BNNT to nitrogen dioxide (NO_2) by the encapsulation of a single Fe atom inside its cavity. The results suggest that the NO_2 molecule can be only physically adsorbed on the pristine BNNT with a small adsorption energy (−0.10 eV). After the inclusion of the Fe atom inside BNNT (Fe@BNNT), the interaction of NO_2 molecules with this tube is significantly enhanced, leading to a transformation from the physisorption of on pristine BNNT to the current chemisorption. Interestingly, up to five NO_2 molecules can be adsorbed on this encapsulated BNNT along its circumference with the average adsorption energy of −0.52 eV, corresponding to a short recovery time (6 ms). Moreover, 0.38 electrons are transferred from the Fe@BNNT to the adsorbed NO_2 molecules, which is enough to induce the obvious change of its electrical conductance. Thus, we predict that the encapsulation of Fe atom inside BNNT would greatly boosts its sensitivity to NO_2 molecules, indicating its potential application as NO_2 sensors.

1. Introduction

As is well-known, nitrogen dioxide (NO_2) is a kind of pungent gas, which is generated in combustion processes. Detection of NO_2 is important due to two main reasons: firstly, it is harmful for human health [1–4] and environment [4–6] because it can cause photochemical smog and acid rain [7,8]. Secondly, NO_2 appears in many industrial processes as it is one of the products of combustion [9–11]. Up to now, several kinds of NO_2 sensors have been developed. Among various NO_2 gas sensing methods which have been proposed, semiconductors [12], solid electrolytes [13], and organic compounds [8] are the most commonly used materials.

The carbon nanotube (CNT), a one dimensional structure with sp^2-hybridized carbon, exhibits many intriguing properties, such as superior electrical conductivity, large surface area, excellent mechanical flexibility, and high thermal/chemical stability [14–16]. These properties render it to have extensive potential applications [17–23], such as solid state sensors [23]. So far, NO_2 adsorption on CNTs has been widely investigated by different research groups [24–34]. For example, Collins [24] and Kong [25] have independently shown that the conductivity of an individual semiconducting CNT increases strongly upon NO_2 gas exposure. Valentini et al. have reported that CNTs could detect NO_2 concentrations as small as 10 ppb [30]. However, since the electronic properties of CNTs are mainly dependent on tabular chirality and diameter [16], separation of CNTs with the desired electronic properties from other kinds is very difficult.

In recent years, semiconductor nanotubes of the type III–V have attracted increasing scientific interest due to their numerous technological applications in nano-engineering, such as optoelectronic devices in the ultraviolet (UV) and visible regions [35–39]. Among them, the boron nitride nanotube (BNNT) [40] is a hotly pursued system, as it shares the same honeycomb lattice structure as CNT. Although they are similar in geometry, BNNT may have more important advantages. For example, BNNT has high thermal conductivity, oxidation resistivity, and thermal and chemical stability [41,42]. Thus, it is one of the most promising materials for nanotechnology applications, especially in oxidative, hazardous, and high temperature environments. In terms of the above unique properties of BNNT, we would like to know the answers of the following questions: (1) whether there is a potential possibility of BNNT serving as a chemical sensor for NO_2 or not; (2) if not, what

* Corresponding authors. Tel.: +86 045188060580.
E-mail addresses: xjz_hmily@yahoo.com.cn, xjz_hmily@163.com (J.-x. Zhao).

http://dx.doi.org/10.1016/j.jmgm.2014.04.005
1093-3263/

is the strategy that can be applied to improve the sensitivity of BNNT to NO_2? Such knowledge may be useful not only to deeply understand the properties of BNNT, but also to develop BNNT-based sensors applied in hazardous and high temperature environments.

2. Computational methods

Calculations were based on the density functional theory (DFT) using the generalized gradient approximation (GGA) for exchange-correlation potential prescribed by Perdew–Burke–Ernzerhof (PBE) [43], which is implemented in DMol^3 package [44,45]. All-electrons calculations were employed with the double numerical basis sets plus polarization functional (DNP), which are comparable to the Gaussian 6-31G(d,p) basis set in size and quality. A zigzag (10, 0) BNNT consisting of 40 boron and 40 nitrogen atoms was considered. One-dimensional (1-D) periodic boundary condition (PBC) was applied along the tube axis to simulate infinitely long (rather than truncated) BNNT systems. Interactions between adsorbed gas molecules and their 1-D periodic images were avoided in our computational supercell models, which include two unit cells of the zigzag tube (for example, supercell length $c = 8.64$ Å for (10, 0) BNNT). The positions of all the atoms in the supercell were fully relaxed during geometry optimizations without any symmetry constraints. Five k-points were used for sampling the 1-D Brillouin zone [46] and the convergence in energy, force, and displacement were set as 10^{-5} ha, 0.002 ha/Å, and 0.005 Å, respectively. The Hirshfeld method [47] was adopted to calculate the charge transfer between adsorbates and BNNTs.

For the Fe-encapsulated BNNT systems in the presence and absence of a NO_2 molecule, the spin-polarized calculations were performed. The adsorption energy of nNO_2 molecules on the pristine or Fe-encapsulated BNNTs is defined as $E_{ads} = [E_{total}(\text{tube} + nNO_2) - E_{total}(\text{tube}) - nE_{total}(NO_2)]/n$, where E_{total} is the energy of the system per supercell and n is the number of the adsorbed NO_2 molecules. By the definition, a negative E_{ads} corresponds to a stable structure. It should be pointed out that we do not consider the correction for basis set superposition error (BSSE) to calculate the adsorption energy because a recent study has proven that the numerical basis sets implemented in Dmol^3 can minimize or even eliminate BSSE [48].

3. Results and discussion

3.1. Pristine single-walled BNNT

First, we study the stable structure of (10, 0) BNNT. As shown in Fig. 1a, two types of B—N bonds can be found: one has the bond length of 1.44 Å and is in parallel with the tube axis, and another has the bond length of 1.45 Å, but is not in parallel with the tube axis. The structural parameters are in good agreement with previous reports [49]. Furthermore, the charge analysis suggests that about 0.20 electrons are transferred from the B atom to its nearest N atoms in the tube, which are much larger than those of carbon nanotubes (CNTs: 0 e). The calculated band structure of the (10, 0) BNNT (Fig. 1b) indicates that it is a direct semiconductor with a band gap of 4.04 eV, in good agreement with previous reports

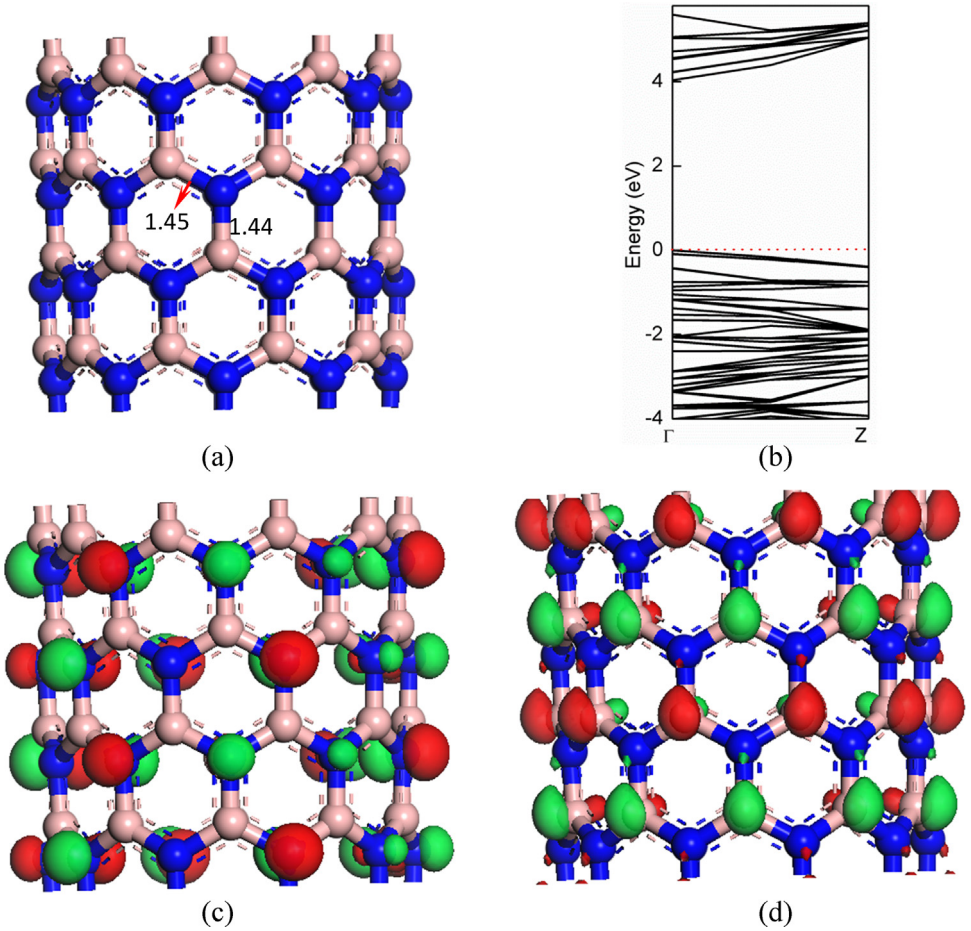

Fig. 1. (a) Optimized structure, (b) band structure, electron density isosurfaces of (c) the highest-energy valence and (d) the lowest-energy conduction of (10, 0) BNNT. The unit of the bond length is Å and the Fermi level is plotted with the red dotted line.

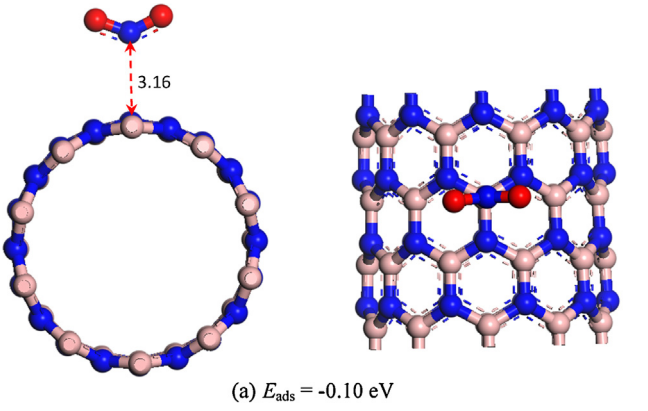

Fig. 2. The obtained stable configurations and the respective adsorption energies of a single NO_2 molecule on the pristine (10, 0) BNNT.

[49]. Based on frontier molecular orbital (FMO) analysis, conduction level mainly originates from the B atoms, while for the valence level mainly originates from the N ones, as shown in Fig. 1c.

3.2. NO_2 adsorption on the pristine BNNT

When the NO_2 molecule is adsorbed on the pristine BNNT, various possible initial configurations are considered, including individual nitrogen or oxygen atoms of NO_2 or both of them close to the boron or nitrogen atom of the BNNT. After fully geometric optimization, only two local minima structures were obtained as shown in Fig. 2. The most stable configuration is such that the N-atom of NO_2 is attached to the B-atom of BNNT, forming a nitro configuration. The calculated adsorption energy is about −0.10 eV and the distance between the adsorbed NO_2 and BNNT is 3.16 Å. This suggests that the NO_2 molecule is only physisorbed on the pristine BNNT. Meanwhile, only 0.03 electrons are transferred from BNNT to NO_2 molecule, which is not enough to change the conductance of BNNT. In this sense, we expect that the pristine BNNT is not suitable as NO_2 sensor.

3.3. NO_2 chemisorption on Fe@BNNTs

Next, the effects of Fe encapsulation on the geometrical structure and electronic properties of the BNNT and also on the sensitivity to NO_2 were investigated. In the current work, we only consider the encapsulation of a single Fe atom inside (10, 0) BNNT (labeled as Fe@BNNT). Initially, the Fe atom is placed near the sidewall of BNNT as shown in Fig. 3a. After full optimization, however, the encapsulated Fe atom spontaneously moves to the center of the tube (Fig. 3b). In this configuration, the shortest distance of the individual Fe atom with the sidewall of BNNT is about 4.07 Å.

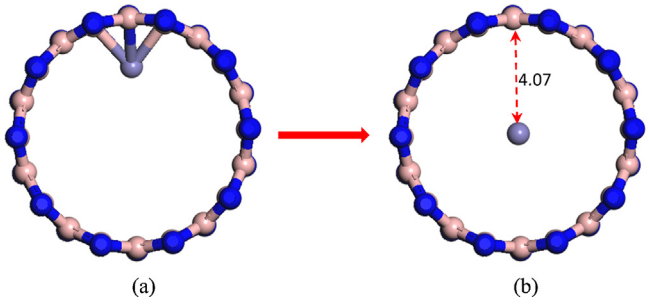

Fig. 3. (a) Initial and (b) optimized structures of the encapsulated (10, 0) BNNT by a single Fe atom. The unit of the bond length is Å.

Moreover, its binding energy (E_b) is −3.16 eV, which is defined as the difference between the total energy of the Fe encapsulated in the BNNT and the sum of the total energies of the corresponding pristine BNNT and the isolated Fe atom. Thus, the encapsulation of the individual Fe atom inside the (10, 0) BNNT is energetically favorable. In addition, about 0.15 electrons are transferred from Fe atom to BNNT. As a result, a net magnetic moment of 4.00 μ_B emerges, which mainly locates on the Fe atom (3.98 μ_B).

Subsequently, we explore the chemisorption of NO_2 molecule on Fe@BNNT. The considered initial configurations are similar to those of on the pristine BNNT. After fully structural relaxation, the obtained stable configurations and the corresponding adsorption energies are displayed in Fig. 4. As shown in Fig. 4a, in the most stable configuration, one O-atom of NO_2 binds with the B-atom of Fe@BNNT, while the other O-atom is pointing to its B_3N_3-hexagonal

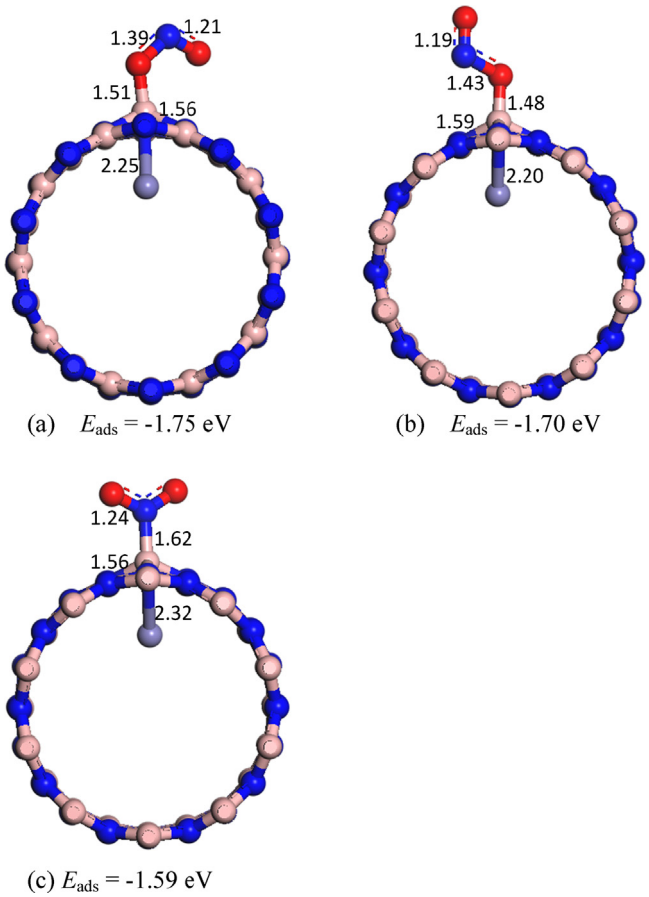

Fig. 4. The obtained stable configurations and the respective adsorption energies of a single NO_2 molecule on Fe@BNNT. The unit of the bond length is Å.

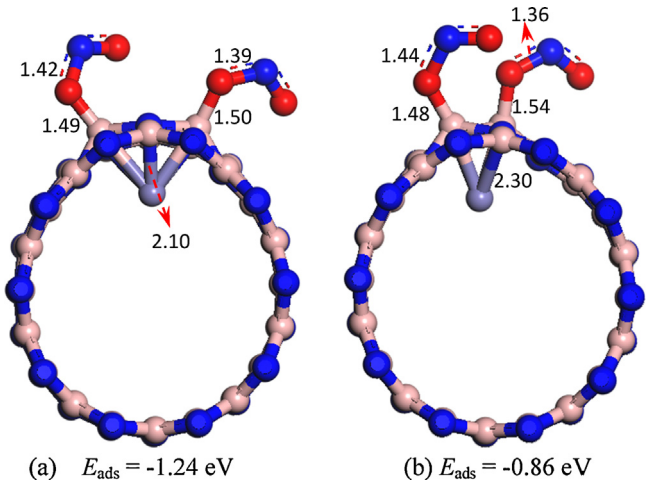

Fig. 5. The obtained stable configurations and the respective average adsorption energies of two NO_2 molecules on Fe@BNNT. The unit of the bond length is Å.

ring. For this nitrite configuration, the newly formed O—B bond is 1.51 Å and the adsorption energy is −1.75 eV. Meanwhile, the amount of charge transfer from NO_2 to BNNT is 0.21 *e*, which is much larger than that of on the pristine BNNT (0.03 *e*). Thus, the chemical reactivity of BNNT toward NO_2 molecule is significantly enhanced due to the encapsulation of an individual Fe atom. Expectably, the strong interaction between the NO_2 molecule and the Fe@BNNT induces a local structural deformation to both NO_2 molecule and BNNT: (1) the bond angle of O—N—O of NO_2 is significantly decreased from 133.5° in free NO_2 to 115.4° in the adsorbed form; (2) the adsorbed B-atom by NO_2 is pulled outward from the tube wall. Such structural deformation is attributed to the change from sp^2 to sp^3 hybridization of the adsorbed B-atom, suggesting that the adsorption is covalent. Notably, the shortest distance between the encapsulated Fe atom and BNNT is shortened by 1.82 Å upon the chemisorption of NO_2 molecule. In addition, two metastable configurations are also obtained as shown in Fig. 4b and c, whose adsorption energies are −1.70 and −1.59 eV, respectively.

With each B-atom on Fe@BNNT being a potential adsorption site, the maximum number of NO_2 molecules is very important to evaluate the possibility of this BNNT as sensor to detect NO_2 molecules. Thus, we further explore the chemisorption of multiple NO_2 molecules on Fe@BNNT. We should point out that only the nitrite configuration is considered on the basis of the results of a single NO_2 molecule adsorption.

When the second NO_2 molecule is chemically adsorbed on the Fe@BNNT on which the first NO_2 molecule is located, the most energetically preferred configuration is that the second NO_2 molecule is adsorbed on the meta-position in the same hexagonal ring along the circumference of the tube (Fig. 5a). The adsorption energy of this configuration is −1.24 eV per NO_2 molecule, which is smaller than that of individual NO_2 molecule (−1.75 eV), and the adsorbed NO_2 molecules exhibit charge transfer of 0.37 *e*. In addition to the lowest-energy configuration, there is the other metastable adsorption configuration, i.e., the configuration with two NO_2 molecules adsorbed on two B-atoms in the same hexagonal ring along the axis of the tube (Fig. 5b, adsorption energy of −0.86 eV per NO_2 molecule).

Based on the above results, more NO_2 molecules are added to the Fe@BNNT one by one. The calculated adsorption configurations are listed in Fig. 6, while the corresponding adsorption energy, geometrical parameters, and charge transfer are given in Table 1. The results show that up to five NO_2 molecules can be stably adsorbed on the encapsulated BNNT by an individual Fe atom. Due to the steric repulsion between NO_2 molecules, it can be expected that

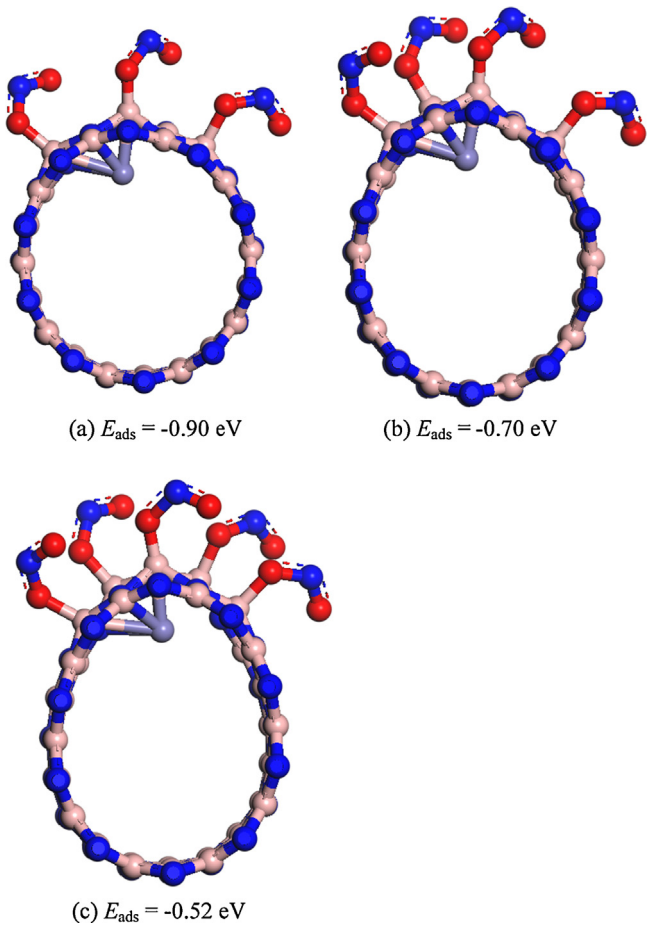

Fig. 6. The obtained stable configurations and the respective average adsorption energies of $n NO_2$ molecules on Fe@BNNT, where *n* is equal to (a) 3, (b) 4, and (c) 5.

the adsorption energy per NO_2 molecule decreases gradually with the increase of the number of adsorbed NO_2 molecules. For the adsorption of five NO_2 molecules, the average adsorption energy is −0.52 eV. Because of the strong interaction between NO_2 molecule and the BNNT, the diameter of BNNT is increased from 7.94 to 9.68 Å after the adsorption of five NO_2 molecules, in which the shortest distance between adsorbates and substrate is about 1.46 Å. In addition, we try to attach more than five NO_2 molecules to this kind of BNNT. Yet, the later NO_2 molecules are found to escape from the tube surface. In other words, the maximum number of NO_2 molecules can be adsorbed on the Fe@BNNT is five ($n_{NO_2} = 5$). To evaluate the effect of dispersion corrections on the chemisorption strength of NO_2 on Fe@BNNT complexes, we further re-calculated the above adsorption energy per NO_2 using Grimme scheme [50]. The results indicate that the average adsorption energies are −2.02 (for $1NO_2$), −1.51 (for $2NO_2$), −1.15 (for $3NO_2$), −0.97 (for $4NO_2$), and −0.80 eV (for $5NO_2$), respectively, which are slightly larger than those of using pure PBE functional (−1.75, −1.24, −0.90, −0.70, and −0.52 eV, respectively). In addition, it is found that the distances between adsorbates and Fe@BNNT are independent on the used methods. Overall, due to the inclusion of a single Fe atom inside BNNT, the interaction of NO_2 with BNNT is changed from physisorption to chemisorption.

Whether a system can serve as an efficient gas sensor depends on its response and recovery time when it is exposed to gaseous molecules [23]. The former is determined by the conductance change induced by charge transfer between detected gases and sensor, while the latter is subjected to the adsorption strength of adsorbates on sensor. To evaluate the possibility of Fe@BNNT as a

Table 1
Structural Parameters, adsorption energies (E_{ads}, eV), and charge transfer (Q, e) for the adsorption of more NO_2 molecules on Fe@BNNT. The units of the bond distance and angle are in angstroms and degrees, respectively.

nNO_2	d(B—N)[a]	d(O—N)[a]	d(O—B)[b]	d(Fe—N)[b]	∠O—N—O[c]	E_{ads} [d]	Q[e]
3	1.62	1.43	1.47	1.95	118.4	−0.90	0.39
4	1.65	1.46	1.45	1.94	118.7	−0.70	0.42
5	1.63	1.44	1.46	1.91	121.5	−0.52	0.38

[a] The largest distance of the given bonds in the bracket.
[b] The shortest distance of the given bonds in the bracket.
[c] The largest bond angles of ∠O—N—O in the adsorbed NO_2 molecules.
[d] The average adsorption energies of nNO_2 molecules on Fe@BNNT.
[e] The sum of charge transfer from Fe@BNNT to adsorbed NO_2 molecules.

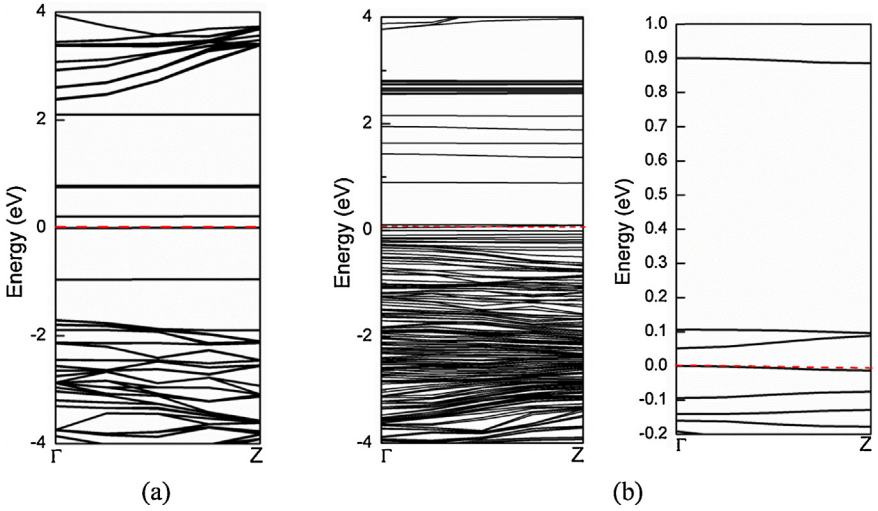

Fig. 7. The band structures of Fe@BNNT (a) before and (b) after adsorption of five NO_2 molecules. The Fermi level is plotted with the red dotted line.

good NO_2 sensor, we therefore discuss the above two questions as follows:

(1) With five NO_2 molecules chemisorbed on the sidewall of Fe@BNNT, the Hirshfeld analysis indicates that the amount of charge transfer from Fe@BNNT to adsorbates is 0.38 e. In order to study the effects of NO_2 adsorption on the electronic properties of Fe@BNNT, its band structures before and after NO_2 adsorption are presented in Fig. 7. For Fe@BNNT, the calculated band gap (E_g) is about 0.21 eV, exhibiting a narrow semiconducting nature as shown in Fig. 7a. This indicates that the band gap of the pristine BNNT (4.04 eV) is greatly decreased due to the encapsulation of the individual Fe atom. Moreover, after the chemisorption of five NO_2 molecules, Fe@BNNT still remains semiconducting nature, while its band gap is decreased to 0.05 eV because certain impurity levels are induced within the band gap of Fe@BNNT as presented in Fig. 7b. It is well known that the electrical conductance of a material is related to its ΔE_g value according to the following equation: $\sigma \propto \exp(-\Delta E_g/2kT)$, where σ is the electrical conductivity and k is the Boltzmann constant [51]. According to the equation, smaller values of ΔE_g at a given temperature lead to larger electrical conductivity. Therefore, the observed decrement (0.16 eV) of E_g for Fe@BNNT in the adsorption process would induce an enhancement for its electrical conductance. In other words, the electronic properties of Fe@BNNT are dramatically changed upon exposure to NO_2 molecules. So we predict that the encapsulation of BNNT with a single Fe may be a good strategy for improving the sensitivity of BNNT to NO_2 molecule. Since the electronic properties of the BNNT are nearly independent of their chirality and diameter [40,52], we believe that the behavior of other types of BNNTs may be similar to this case.

(2) As an ideal gas sensor, it should exhibit quick recovery time. Commonly, the stronger interactions imply that desorption of the adsorbate could be difficult and the device may suffer from long recovery times. If E_{ads} is significantly increased, much longer recovery time is expected. Based on the conventional transition state theory [53], the recovery time of Fe@BNNT-based NO_2 sensor at room temperature is roughly estimated to be 6 ms at the adsorption energy of −0.52 eV (for five NO_2 molecules), according to the formula, $\tau = \nu_0^{-1} \exp(-E_{ads}/K_B T)$, where T is temperature, K_B the Boltzmann's Constant (8.62×10^{-5} eV K^{-1}), and ν_0 is the attempt frequency ($\nu_0 = 10^{12}$ s^{-1} for NO_2 [54]). Therefore, the encapsulated BNNT by a single Fe atom should be good NO_2 sensors with short recovery time. It should be noted that the encapsulation of Fe clusters and nanowires/nanorods has been achieved both experimentally [55,56] and theoretically [57–59]. If more Fe atoms are encapsulated inside BNNT, more atoms in BNNT might be "activated". Then, the number of adsorbed NO_2 molecules on BNNT should be greatly increased. Thus, the sensitivity of this BNNT to NO_2 molecules would be inevitably enhanced and the corresponding study on the above questions is still underway.

4. Conclusions

In summary, we have explored the adsorption of NO_2 molecules on the pristine and Fe-encapsulated BNNTs by performing DFT calculations. The results indicate that the NO_2 molecule can only physically interact with the pristine BNNT via van der Waals forces, but it exhibits much stronger attachment to the Fe-encapsulated BNNT. Up to five NO_2 molecules can be chemisorbed on the outer sidewall of Fe@BNNT with the charge transfer of 0.38 e from the

tube to NO_2 molecules, which would be enough to induce the conductance change of the tube. Moreover, the calculated adsorption energy (−0.52 eV) per NO_2 molecule corresponds to a short recovery time of 6 ms at room temperature. The present results are expected to provide a useful guidance to develop novel BNNT-based sensors for the detection of toxic NO_2 with quick response and short recovery time.

Acknowledgments

This work is supported by the National Nature Science Foundation of China (No. 21203048) and Scientific Research Fund of Heilongjiang Provincial Education Department (No. 12531195). The authors would like to show great gratitude to the reviewers for raising invaluable comments and suggestions.

References

[1] R. Ehrlich, M.C. Henry, Chronic toxicity of nitrogen dioxide. I. Effect on resistance to bacterial pneumonia, J. Occup. Med. 12 (1970) 34.
[2] K. Mukala, J. Pekkanen, P. Tiittanen, S. Alm, R. Salonen, J. Tuomisto, Personally measured weekly exposure to NO_2 and respiratory health among preschool children, Eur. Respir. J. 13 (1999) 1411–1417.
[3] R.L. Tse, A.A. Bockman, Nitrogen dioxide toxicity report of four cases in firemen, J. Am. Med. Assoc. 212 (1970) 1341–1344.
[4] Nitrogen Dioxide – Wikipedia, The Free Encyclopedia, 2011, http://en.wikipedia.org/wiki/Nitrogen dioxide
[5] Z. Ross, P.B. English, R. Scalf, R. Gunier, S. Smorodinsky, S. Wall, M. Jerrett, Nitrogen dioxide prediction in southern California using land use regression modeling: potential for environmental health analyses, J. Expo. Sci. Environ. Epidemiol. 16 (2005) 106–114.
[6] Health Aspects of Air Pollution with Particulate Matter, Ozone and Nitrogen Dioxide, 2003, http://www.euro.who.int/document/e79097.pdf
[7] Y. Sadaoka, T.A. Jones, G.S. Revell, W. Göpel, Effects of morphology on NO_2 detection in air at room temperature with phthalocyanine thin films, J. Mater. Sci. 25 (1990) 5257–5268.
[8] N.O. Korolkoff, Survey of toxic gas sensors and monitoring systems, Solid State Technol. 32 (1989) 49–64.
[9] N. Docquier, S. Candel, Combustion control and sensors: a review, Prog. Energy Combust. Sci. 28 (2002) 107–150.
[10] G. Guillaud, J. Simon, J. Germain, Metallophthalocyanines: gas sensors, resistors and field effect transistors, Coord. Chem. Rev. 178–180 (1998) 1433–1484.
[11] P. Moseley, Solid state gas sensors, Meas. Sci. Technol. 8 (1997) 223–237.
[12] G. Sberveglieri, S. Groppelli, P. Nelli, Highly sensitive and selective NO_x and NO_2 sensor based on Cd-doped SnO_2 thin films, Sens. Actuators B: Chem. 4 (1991) 457–461.
[13] M.L. Grilli, E.D. Bartolomeo, E. Traversa, Electrochemical NO_x sensors based on interfacing nanosized $LaFeO_3$ perovskite-type oxide and ionic conductors, J. Electrochem. Soc. 148 (2001) H98–H102.
[14] J.W.G. Wilder, L.C. Venema, A.G. Rinzler, R.E. Smalley, C. Dekker, Electronic structure of atomically resolved carbon nanotubes, Nature 391 (1998) 59–62.
[15] R.H. Bauhman, A.A. Zakhidov, W.A. de Heer, Carbon nanotubes—the route toward applications, Science 297 (2002) 787–792.
[16] J.C. Charlier, Defects in carbon nanotubes, Acc. Chem. Res. 35 (2002) 1063–1069.
[17] A. Javey, J. Guo, Q. Wang, M. Lundstrom, H. Dai, Ballistic carbon nanotube field-effect transistors, Nature 424 (2003) 654–657.
[18] L. Minati, G. Speranza, I. Bernagozzi, S. Torrengo, L. Toniutti, B. Rossi, M. Ferrari, A. Chiasera, Investigation on the electronic and optical properties of short oxidized multiwalled carbon nanotubes, J. Phys. Chem. C 114 (2010) 11068–11073.
[19] X. Pan, Z. Fan, W. Chen, Y. Ding, H. Luo, X. Bao, Enhanced ethanol production inside carbon-nanotube reactors containing catalytic particles, Nat. Mater. 6 (2007) 507–511.
[20] X. Yang, Z. Zhou, D. Wang, X. Liu, High sensitivity carbon nanotubes flow-rate sensors and their performance improvement by coating, Sensors 10 (2010) 4898–4906.
[21] C. Liu, Y.Y. Fan, M. Liu, H.T. Cong, H.M. Cheng, M.S. Dresselhaus, Hydrogen storage in single-walled carbon nanotubes at room temperature, Science 286 (1999) 1127–1129.
[22] M. Kibalchenko, M.C. Payne, J.R. Yates, Magnetic response of single-walled carbon nanotubes induced by an external magnetic field, ACS Nano 5 (2011) 537–545.
[23] P. Bondavalli, P. Legagneux, D. Pribat, Carbon nanotubes based transistors as gas sensors: state of the art and critical review, Sens. Actuators B: Chem. 140 (2009) 304–318.
[24] P.G. Collins, K. Bradley, M. Ishigami, A. Zettl, Extreme oxygen sensitivity of electronic properties of carbon nanotubes, Science 287 (2000) 1801–1804.
[25] J. Kong, N.R. Franklin, C. Zhou, M.G. Chapline, S. Peng, K. Cho, H. Dai, Nanotube molecular wires as chemical sensors, Science 287 (2000) 622–625.
[26] L. Bai, Z. Zhou, Computational study of B- or N-doped single-walled carbon nanotubes as NH_3 and NO_2 sensors, Carbon 45 (2007) 2105–2110.
[27] S. Peng, K. Cho, Chemical control of nanotube electronic, Nanotechnology 11 (2000) 57–61.
[28] T. Zhu, B.G. Shen, J.R. Sun, H.W. Zhao, W.S. Zhan, Surface spin-glass behavior in $La_{2/3}Sr_{1/3}MnO_3$ nanoparticles, Appl. Phys. Lett. 78 (2001) 3863–3865.
[29] L. Valentini, F. Mercuri, I. Armentano, C. Cantalini, S. Picozzi, L. Lozzi, S. Santucci, A. Sgamellotti, J.M. Kenny, Role of defects on the gas sensing properties of carbon nanotubes thin films: experiment and theory, Chem. Phys. Lett. 387 (2004) 356–361.
[30] L. Valentini, I. Armentano, J.M. Kenny, C. Cantalini, L. Lozzi, S. Santucci, Sensors for sub-ppm NO_2 gas detection based on carbon nanotube thin films, Appl. Phys. Lett. 82 (2003) 961–963.
[31] S. Santucci, S. Picozzi, F. Di Gregorio, L. Lozzi, C. Cantalini, L. Valentini, J.M. Kenny, B. Delley, NO_2 and CO gas adsorption on carbon nanotubes: experiment and theory, J. Chem. Phys. 119 (2003) 10904–10910.
[32] K. Seo, K.A. Park, C. Kim, S. Han, B. Kim, Y.H. Lee, Chirality- and diameter-dependent reactivity of NO_2 on carbon nanotube walls, J. Am. Chem. Soc. 127 (2005) 15724–15729.
[33] Y. Zhang, C. Suc, Z. Liu, J. Li, Carbon nanotubes functionalized by NO_2: coexistence of charge transfer and radical transfer, J. Phys. Chem. B 110 (2006) 22462–22470.
[34] W.L. Yim, X.G. Gong, Z.F. Liu, Chemisorption of NO_2 on carbon nanotubes, J. Phys. Chem. B 107 (2003) 9363–9369.
[35] M. Machado, R. Mota, P. Piquini, Electronic properties of BN nanocones under electric fields, Microelectron. J. 34 (2003) 545–547.
[36] J.B. Halpern, A. Bello, J. Gilcrease, G.L. Harris, M. He, Biphasic GaN nanowires: growth mechanism and properties, Microelectron. J. 40 (2009) 316–318.
[37] J. Beheshtian, M. Kamfiroozi, Z. Bagheri, A.A. Peyghan, $B_{12}N_{12}$ nano-cage as potential sensor for NO_2 detection, Chin. J. Chem. Phys. 25 (2012) 60–64.
[38] J. Beheshtian, Z. Bagheri, M. Kamfiroozi, A. Ahmadi, Toxic CO detection by $B_{12}N_{12}$ nanocluster, Microelectron. J. 42 (2011) 1400–1403.
[39] J. Beheshtian, M. Kamfiroozi, Z. Bagheri, A. Ahmadi, Theoretical study of hydrogen adsorption on the $B_{12}P_{12}$ fullerene-like nanocluster, Comput. Mater. Sci. 54 (2012) 115–118.
[40] A. Rubio, J.L. Corkill, M.L. Cohen, Theory of graphitic boron nitride nanotubes, Phys. Rev. B 49 (1994) 5081–5084.
[41] D. Golberg, Y. Bando, C.C. Tang, C.Y. Zhi, Boron nitride nanotubes, Adv. Mater. 19 (2007) 2413–2432.
[42] C. Zhi, Y. Bando, C. Tang, D. Golberg, Boron nitride nanotubes, Mater. Sci. Eng. R: Rep. 70 (2010) 92–111.
[43] J.P. Perdew, K. Burke, M. Ernzerhof, Generalized gradient approximation made simple, Phys. Rev. Lett. 77 (1996) 3865–3868.
[44] B. Delley, An all-electron numerical method for solving the local density functional for polyatomic molecules, J. Chem. Phys. 92 (1990) 508–517.
[45] B. Delley, From molecules to solids with the $DMol^3$ approach, J. Chem. Phys. 113 (2000) 7756–7764.
[46] H.J. Monkhorst, J.D. Pack, Special points for Brillouin-zone integrations, Phys. Rev. B 13 (1976) 5188–5192.
[47] F.L. Hirshfeld, Bonded-atom fragments for describing molecular charge densities, Theor. Chim. Acta 44 (1977) 129–138.
[48] Y. Inada, H. Orita, Efficiency of numerical basis sets for predicting the binding energies of hydrogen bonded complexes: evidence of small basis set superposition error compared to Gaussian basis sets, J. Comput. Chem. 29 (2007) 225–232.
[49] Q. Wang, Y.J. Liu, J.X. Zhao, Theoretical study on the encapsulation of Pd_3-based transition metal clusters inside boron nitride nanotubes, J. Mol. Model. 19 (2013) 1143–1151.
[50] S. Grimme, Semiempirical GGA-type density functional constructed with a long-range dispersion correction, J. Comput. Chem. 27 (2006) 1787–1799.
[51] S.S. Li, Semiconductor Physical Electronics, 2nd ed., Springer, USA, 2006.
[52] G.G. Fuentes, E. Borowiak-Palen, T. Pichler, X. Liu, A. Graff, G. Behr, R.J. Kalenczuk, M. Knupfer, J. Fink, Electronic structure of multiwall boron nitride nanotubes, Phys. Rev. B 67 (2003) 035429–035434.
[53] J. Beheshtian, A.A. Peyghan, Z. Bagheri, Detection of phosgene by Sc-doped BN nanotubes: a DFT study, Sens. Actuators B: Chem. 171–172 (2012) 846–852.
[54] S. Peng, K. Cho, P. Qi, H. Dai, Ab initio study of CNT NO_2 gas sensor, Chem. Phys. Lett. 387 (2004) 271–276.
[55] T. Oku, I. Narita, H. Tokoro, Synthesis and magnetic property of boron nitride nanocapsules encaging iron and cobalt nanoparticles, J. Phys. Chem. Solids 67 (2006) 1152–1156.
[56] D. Golberg, F.F. Xu, Y. Bando, Filling boron nitride nanotubes with metals, Appl. Phys. A: Mater. Sci. Process. 76 (2003) 479–485.
[57] J.M. Zhang, S.F. Wang, X.J. Du, K.W. Xu, V. Ji, Comparison of electronic and magnetic properties of Fe, Co, and Ni nanowires encapsulated in boron nitride nanotubes, J. Phys. Chem. C 113 (2009) 17745–17750.
[58] S.F. Wang, J.M. Zhang, K.W. Xu, Structural, electronic and magnetic properties of Fe nanowires encapsulated in boron nitride nanotubes, Phys. B: Condens. Matter 405 (2010) 1035–1039.
[59] Y. Xie, J.M. Zhang, Structural, electronic and magnetic properties of $Fe_{(1-x)}Co_x$ alloy nanowires encapsulated inside (10, 0) boron nitride nanotube, J. Phys. Chem. Solids 73 (2012) 530–534.